Int. J. Heat Mass Transfer. Vol. 23, pp. 789–798

0017-9310/80/0601-0789 $02.00/0

VORTEX INSTABILITY OF MIXED CONVECTIVE FLOW IN A SEMI-INFINITE POROUS MEDIUM BOUNDED BY A HORIZONTAL SURFACE

C. T. HSU

Fluid Mechanics Department, DSSG of TRW, Inc., One Space Park, Redondo Beach, CA 90278, U.S.A.

and

PING CHENG

Department of Mechanical Engineering, University of Hawaii, Honolulu, HI 96822, U.S.A.

(*Received* 5 *September* 1979 *and in revised form* 7 *November* 1979)

Abstract — A linear stability analysis is performed to determine the conditions marking the onset of longitudinal vortices in mixed convective flows in a semi-infinite porous medium adjacent to a horizontal impermeable surface. Two different aiding flows are considered: (1) flow past a horizontal impermeable surface with zero angle of incidence, and (2) stagnation point flow about a horizontal surface. For each problem, the basic state is assumed to be the steady two-dimensional boundary layer flow which is characterized by non-linear velocity and temperature profiles. The transient three-dimensional disturbances equations are simplified based on a scaling argument, and the resulting simplified equations are solved based on the local similarity method. The critical Peclet numbers and the associated wave numbers as a function of the mixed convection parameter for the two cases are obtained. For the vortex mode of instability, it is found that the stagnation point flow is more stable than the case of the horizontal aiding flow for the same value of the mixed convection parameter. In both cases, the effect of the external aiding flow is to suppress the onset of vortex instability in the porous layer adjacent to the horizontal bounding surface.

NOMENCLATURE

a, dimensionless spanwise wave number;
a_i, lower limits in the integrals in equation (64);
A, constant in wall temperature relation;
A_0, integration constant in equation (56);
B, constant in free stream velocity;
B_0, integration constant in equation (54);
C_i, superposition constant;
D, differentiation with respect to disturbances;
D_v, parabolic cylinder function of order v;
f, dimensionless base state stream function;
F, dimensionless disturbance stream function;
g, acceleration due to gravity;
G, dimensionless disturbance velocity in the x-direction;
i, complex number;
k, dimensionless wave number for mixed convection;
k_f, dimensionless wave number for free convection;
K, Darcy permeability;
m, exponent on wall temperature relation;
M, mixed convection parameter;
n, exponent on free stream velocity;
p, pressure;
P, dimensionless pressure;
Pe, local Peclet number;
Pe_l, Peclet number based on the characteristic length;
Ra_x, local Rayleigh number;
Ra_l, Rayleigh number based on the characteristic length;
t, time;
T, temperature;
u, Darcy's velocity in x-direction;
U, dimensionless Darcy's velocity in x-direction;
v, Darcy's velocity in y-direction;
V, dimensionless Darcy's velocity in y-direction;
w, Darcy's velocity in z-direction;
W, dimensionless Darcy's velocity in z-direction;
x, dimensional coordinate in downstream direction;
X, dimensionless coordinate in downstream direction;
y, dimensional coordinate normal to bounding surface;
Y, dimensionless coordinate normal to bounding surface;
z, dimensional coordinate tangent to bounding surface;
Z, dimensionless coordinate tangent to bounding surface.

Greek symbols

α, effective thermal diffusivity;
β, coefficient of thermal expansion;
δ_T, thermal boundary layer thickness;
ε, $\varepsilon = (Pe_l)^{-1/2}$;
γ, volumetric heat capacity of the fluid to that of the saturated porous medium;
Γ, gamma function;

Δ, function defined in equation (70);
μ, fluid viscosity;
ξ, independent variable in equation (55);
η, similarity variable;
θ, dimensionless base state temperature;
Θ, dimensionless disturbance temperature;
ψ, stream function;
ρ, fluid density;
τ, dimensionless time.

Superscripts

$\hat{}$, amplitude function for disturbances;
$*$, critical values;
$\tilde{}$, dimensionless quantities.

Subscripts

0, basic undisturbed quantities;
1, disturbed quantities;
∞, condition away from the bounding surface;
w, condition at the wall.

1. INTRODUCTION

THE PROBLEMS of onset of cellular convection in a porous medium has received considerable attention in the last decade because of its applications to the transport processes occurring in geothermal reservoirs (see Witherspoon *et al.*[1] and Cheng[2] for a review of literature). A linear stability analysis was performed by Lapwood[3] to study the onset of cellular convection in a porous medium bounded by two parallel horizontal impermeable surfaces heated from below. Lapwood's work was subsequently extended by Katto and Masuoka[4], Kassoy and Zebib[5], and by Walker and Homsy[6], among others. Beck[7] considered the effects of lateral walls on the onset of cellular convection in an enclosed three-dimensional porous medium heated from below. The effects of inclination angle on the onset of longitudinal rolls in a porous medium bounded by parallel plates heated from below was investigated by Bories and Combarnous[8]. The effects of vertical through flow on the onset of cellular convection in a porous medium heated from below have been studied by Wooding[9], Sutton[10], and by Homsy and Sherwood[11]. The onset of cellular convection in a porous medium bounded by two vertical impermeable surfaces with differential heating was investigated by Gill[12]. In all of these problems, the basic states are either motionless or one-dimensional uniform flow with temperature profiles depending on one spatial coordinate.

Little work has been done, however, on the problems of thermal instability in boundary layer flows in a porous medium adjacent to a heated or cooled impermeable surface, where the basic flow is characterized by non-parallel, two-dimensional profiles. In a recent paper, Hsu, Cheng and Homsy[13] investigated the conditions marking the onset of vortex instability in free convection boundary layer flows in a porous medium adjacent to a horizontal surface. The occurrence of this form of instability is owing to the destabilizing effects of the component of buoyancy force normal to the surface. In the present paper, the effects of external aiding flows on the onset of vortex instability in mixed convection in a porous medium adjacent to horizontal surfaces will be studied. Two cases with different external aiding flows will be considered: (1) flow past a horizontal impermeable surface with constant heat flux at zero angle of incidence, and (2) stagnation point flow about a horizontal impermeable surface with $T_w \propto x^2$. The approach adopted in the present paper is similar to the previous work by Hsu, Cheng and Homsy[13] as well as by Hsu and Cheng[14], wherein the three-dimensional disturbances are not assumed to be independent of streamwise direction *a priori*. This represents a major departure from the quasi-parallel models adopted in the earlier work on the corresponding problems in a viscous fluid[15, 16]. Instead, the governing equations for the three-dimensional disturbances are simplified based on a scaling argument. As a result, the disturbances at the onset of vortex instability are shown to be confined within the boundary layer of the basic flow, which is consistent with the assumption of "bottling effects" invoked by Haaland and Sparrow[15]. The simplified equations suggest the existence of a stream function for the secondary flow and the resulting equations admit a local similarity solution that lead to an eigenvalue problem. The critical Peclet numbers and the associated wave numbers as a function of the mixed convection parameter $Ra/(Pe)^{3/2}$ for the two cases are obtained. It is found that the effect of the external aiding flow is to suppress the onset of vortex instability in the porous layer adjacent to the horizontal surface.

2. LINEAR STABILITY ANALYSIS

Consider the problems of steady mixed convection in a semi-infinite porous medium bounded by a horizontal impermeable surface for the two situations shown in Fig. 1, where the coordinates x and z are placed on the bounding surface with the coordinate y pointing vertically toward the porous medium. Figs. 1 (a) and (c) represent the case of external flow past heated and cooled surfaces at zero angle of incidence, while Figs. 1(b) and (d) represent the case of stagnation point flow about heated and cooled horizontal surfaces. The free stream velocity can be represented by $u_\infty = Bx^n$ (with $n = 0$ denoting the former case and $n = 1$ for the latter case). If the boundary layer thickness, δ_T, is thin, and if Darcy's law is applicable, it has been shown that similarity solutions exist for the former problem if $T_w \propto x^{1/2}$ (the constant heat flux solution) and for the latter problem if $T_w \propto x^2$[17]. The solutions are of the form

$$T_0(x, y) = T_w + Ax^m\theta_0(\eta), \tag{1}$$

$$\psi_0(x, y) = \alpha\sqrt{(Pe)}f_0(\eta), \tag{2}$$

$$\eta = \sqrt{(Pe)}\,y/x, \tag{3}$$

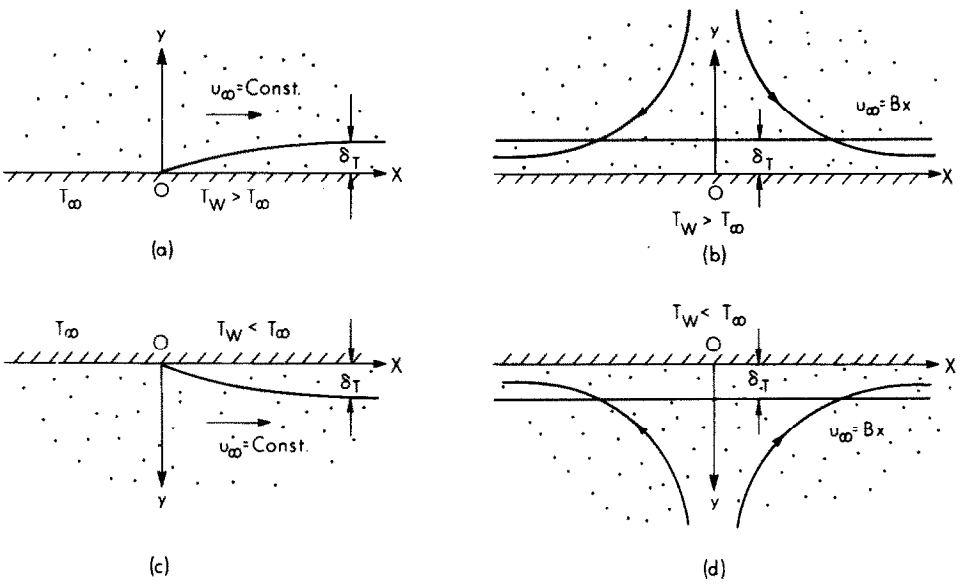

FIG. 1. Coordinate systems.

where $Pe = u_\infty x/\alpha$ is the Peclet number and $m = (3n + 1)/2$ (thus $m = 1/2, 2$ for $n = 0$ and 1); $\theta_0(\eta)$ and $f_0(\eta)$ are the dimensionless temperature and stream function determined from

$$f_0'' = -M\left[m\theta_0 + \left(\frac{m-2}{3}\right)\eta\theta_0'\right], \tag{4}$$

$$\theta_0'' = m\theta_0 f_0' - \left(\frac{m+1}{3}\right) f_0\theta_0', \tag{5}$$

subject to the boundary conditions

$$\theta_0(0) = 1, \qquad f_0(0) = 0, \tag{6a, b}$$

$$\theta_0(\infty) = 0, \qquad f_0'(\infty) = 1, \tag{7a, b}$$

where

$$M \equiv Ra/(Pe)^{3/2} = \frac{\rho_\infty g\beta KA}{\mu B}(\alpha/B)^{1/2}$$

is a constant independent of x, which is the governing parameter for mixed convection in a porous medium adjacent to horizontal surfaces. For the case of forced convection, i.e. $M = 0$, equations (4) and (5) with boundary conditions equations (6) and (7) have the exact solution of the form

$$f_0 = \eta, \tag{8}$$

$$\theta_0 = \left[\frac{\Gamma\left(\frac{1-\nu}{2}\right)}{2^{\nu/2}\Gamma\left(\frac{1}{2}\right)}\right] \exp(\tilde{\xi}^2/4) D_\nu(\tilde{\xi}), \tag{9}$$

where $\tilde{\xi} \equiv \sqrt{[(m+1)/3]}\eta$ and $D_\nu(\tilde{\xi})$ is the parabolic cylinder function [18] of order ν where $\nu \equiv -[(4m+1)/(m+1)]$.

A linear stability analysis will now be performed to investigate the instability of the boundary layer flow as given by equations (1)–(7). To this end, the physical variables will now be decomposed into basic and infinitesimal disturbed quantities as

$$\begin{aligned} T(x, y, z, t) &= T_0(x, y) + T_1(x, y, z, t), \\ p(x, y, z, t) &= p_0(x, y) + p_1(x, y, z, t), \\ u(x, y, z, t) &= u_0(x, y) + u_1(x, y, z, t), \\ v(x, y, z, t) &= v_0(x, y) + v_1(x, y, z, t), \\ w(x, y, z, t) &= w_1(x, y, z, t). \end{aligned} \tag{10}$$

Substituting equation (10) into the governing equations for transient three-dimensional convective flow in a porous medium, subtracting the boundary layer equations for the basic undisturbed flow, and after linearizing yields

$$\frac{\partial u_1}{\partial x} + \frac{\partial v_1}{\partial y} + \frac{\partial w_1}{\partial z} = 0, \tag{11}$$

$$u_1 = -\frac{K}{\mu}\frac{\partial p_1}{\partial x}, \tag{12}$$

$$v_1 = -\frac{K}{\mu}\left(\frac{\partial p_1}{\partial y} - \rho_\infty g\beta T_1\right), \tag{13}$$

$$w_1 = -\frac{K}{\mu}\frac{\partial p_1}{\partial z}, \tag{14}$$

$$\gamma\frac{\partial T_1}{\partial t} + u_0\frac{\partial T_1}{\partial x} + v_0\frac{\partial T_1}{\partial y} + u_1\frac{\partial T_0}{\partial x} + v_1\frac{\partial T_0}{\partial y} = \alpha\left(\frac{\partial^2 T_1}{\partial x^2} + \frac{\partial^2 T_1}{\partial y^2} + \frac{\partial^2 T_1}{\partial z^2}\right). \tag{15}$$

Some of the x-derivative terms in equations (11)–(15) will now be shown to be smaller than other terms in the same equation and thus can be neglected. To this

end, we first recast the disturbances equations in the length scale of the basic flow, i.e.

$$X = x/l \quad \text{and} \quad Y = y/\varepsilon l, \tag{16a, b}$$

where $\varepsilon = (Pe_l)^{-1/2}$ and $Pe_l = u_r l/\alpha$ is the Peclet number based on the characteristic length l. The basic flow quantities will also be rescaled as

$$U_0 = \frac{\varepsilon^2 l u_0}{\alpha}, \quad V_0 = \frac{\varepsilon l v_0}{\alpha}, \quad \text{and} \quad \Theta_0 = \frac{T_0}{\Delta T_r}, \tag{17a, b, c}$$

so that U_0, V_0, and Θ_0 as well as their derivatives with respect to X and Y are of $O(1)$ (see [17]). For vortex-roll disturbances, z and y are of the same scale; thus, according to equation (16b), we have

$$Z = z/\varepsilon l. \tag{18}$$

The disturbance velocity v_1 from equation (13) is of $O(Ra_l)$ if

$$\Theta_1 = \frac{T_1}{\Delta T_r}, \tag{19}$$

where $\Delta T_r = Al^m$ and $Ra_l = K\rho_r g\beta \Delta T_r l/\mu\alpha$ is the Rayleigh number based on l. Since the similarity of the basic flow requires that $M = Ra_l/(Pe_l)^{3/2}$ to be a constant, we have $v_1 = O(Ra_l) = O(\varepsilon^{-3})$ which follows from equation (13). Consequently, we have

$$V_1 = \frac{\varepsilon^3 l v_1}{\alpha}, \quad W_1 = \frac{\varepsilon^3 l w_1}{\alpha},$$

$$U_1 = \frac{\varepsilon^2 l u_1}{\alpha}, \quad \text{and} \quad P_1 = \frac{\varepsilon^2 K p_1}{\mu\alpha}. \tag{20}$$

The disturbance equations in terms of the new dimensionless variables are

$$\varepsilon^2 \frac{\partial U_1}{\partial X} + \frac{\partial V_1}{\partial Y} + \frac{\partial W_1}{\partial Z} = 0, \tag{21}$$

$$U_1 = -\frac{\partial P_1}{\partial X}, \tag{22}$$

$$V_1 = -\frac{\partial P_1}{\partial Y} + M\Theta_1, \tag{23}$$

$$W_1 = -\frac{\partial P_1}{\partial Z}, \tag{24}$$

$$\varepsilon^2 \frac{\partial^2 \Theta_1}{\partial X^2} + \left(\frac{\partial^2 \Theta_1}{\partial Y^2} + \frac{\partial^2 \Theta_1}{\partial Z^2}\right) = \frac{\partial \Theta_1}{\partial \tau} + U_0 \frac{\partial \Theta_1}{\partial X} + V_0 \frac{\partial \Theta_1}{\partial Y} + U_1 \frac{\partial \Theta_0}{\partial X} + \frac{V_1}{\varepsilon^2} \frac{\partial \Theta_0}{\partial Y}, \tag{25}$$

where $\tau = \alpha t/\gamma l^2 \varepsilon^2$. The first terms in equations (21) and (25) are the smallest terms in their respective equations and can therefore be neglected. Note that the last term $(V_1/\varepsilon^2)(\partial\Theta_0/\partial Y)$ in equation (25), however, is larger than other terms by $O(1/\varepsilon^2)$. This means that (X, Y, Z) as defined in equations (16) and (18) may not be the right length scale for the disturbances. From equation (25), Y and Z have to be rescaled to

$$\tilde{Y} = Y/\varepsilon, \quad \tilde{Z} = Z/\varepsilon. \tag{26}$$

We also need to rescale X into

$$\tilde{X} = X/\varepsilon, \tag{27}$$

in order to preserve the similarity characteristics between (y, z) and x. From equation (24), a proper scale for P_1 is

$$\tilde{P}_1 = P_1/\varepsilon. \tag{28}$$

In terms of $(\tilde{X}, \tilde{Y}, \tilde{Z})$ and $\tilde{P}_1$, equations (21)–(25) become

$$\varepsilon^2 \frac{\partial U_1}{\partial \tilde{X}} + \frac{\partial V_1}{\partial \tilde{Y}} + \frac{\partial W_1}{\partial \tilde{Z}} = 0, \tag{29}$$

$$U_1 = -\frac{\partial \tilde{P}_1}{\partial \tilde{X}}, \tag{30}$$

$$V_1 = -\frac{\partial \tilde{P}_1}{\partial \tilde{Y}} + M\Theta_1, \tag{31}$$

$$W_1 = -\frac{\partial \tilde{P}_1}{\partial \tilde{Z}}, \tag{32}$$

and

$$\varepsilon^2 \frac{\partial^2 \Theta_1}{\partial \tilde{X}^2} + \left(\frac{\partial^2 \Theta_1}{\partial \tilde{Y}^2} + \frac{\partial^2 \Theta_1}{\partial \tilde{Z}^2}\right) = \frac{\partial \Theta_1}{\partial \tilde{\tau}} + \varepsilon U_0 \frac{\partial \Theta_1}{\partial \tilde{X}} + \varepsilon V_0 \frac{\partial \Theta_1}{\partial \tilde{Y}} + \varepsilon^2 U_1 \frac{\partial \Theta_0}{\partial X} + V_1 \frac{\partial \Theta_0}{\partial Y}, \tag{33}$$

where $\tilde{\tau} = \tau/\varepsilon^2$. Note that in equation (33) no rescaling for the terms $\partial\Theta_0/\partial X$ and $\partial\Theta_0/\partial Y$ is required because these terms are the derivatives of the basic flow quantities which are already of $O(1)$.

We observe that (i) the rescaling of (X, Y, Z) into $(\tilde{X}, \tilde{Y}, \tilde{Z})$ suggests that the disturbances are confined in a length scale which is of $O(\varepsilon)$ smaller than the length scale of the basic flow; this confirms the "bottling effect" of Haaland and Sparrow[15]; (ii) the omission of the terms $\partial u_1/\partial x$ and $\alpha(\partial^2 T_1/\partial x^2)$ in equations (11) and (15), respectively, is consistent with the level of approximation of the basic flow. Note that although the term $u_1(\partial T_0/\partial x)$ is of the same order as $\alpha(\partial^2 T_1/\partial x^2)$ in the length scale $(\tilde{X}, \tilde{Y}, \tilde{Z})$ as seen from equation (33), $u_1(\partial T_0/\partial x)$ will be retained in the numerical computations because it is of the same order with other convective terms in the scale of the basic flow [see equation (25)], and the inclusion of this term does not hinder further analysis as we shall see.

We now return to equations (11)–(15) with the terms $\partial u_1/\partial x$ and $\alpha(\partial^2 T_1/\partial x^2)$ neglected. The omission of $\partial u_1/\partial x$ in equation (11) implies the existence of a stream function ψ_1 for the secondary flow such that

$$w_1 = \frac{\partial \psi_1}{\partial y} \quad \text{and} \quad v_1 = -\frac{\partial \psi_1}{\partial z}. \tag{34}$$

Eliminating p_1 from equations (12)–(14), and with the

aid of equation (34), leads to

$$\frac{\partial u_1}{\partial z} = \frac{\partial^2 \psi_1}{\partial x \partial y}, \tag{35}$$

$$\frac{\partial^2 \psi_1}{\partial y^2} + \frac{\partial^2 \psi_1}{\partial z^2} = -\frac{\rho_\infty \beta g K}{\mu} \frac{\partial T_1}{\partial z}. \tag{36}$$

Equation (15) in terms of stream function ψ_1 and with the streamwise heat conduction term neglected is

$$\gamma \frac{\partial T_1}{\partial t} + u_0 \frac{\partial T_1}{\partial x} + v_0 \frac{\partial T_1}{\partial y} + u_1 \frac{\partial T_0}{\partial x} - \frac{\partial \psi_1}{\partial z} \frac{\partial T_0}{\partial y} = \alpha \left(\frac{\partial^2 T_1}{\partial y^2} + \frac{\partial^2 T_1}{\partial z^2} \right), \tag{37}$$

where

$$u_0 = \frac{\partial \psi_0}{\partial y} = \frac{\alpha}{x} Pe\, f_0'(\eta)$$

and

$$v_0 = -\frac{\partial \psi_0}{\partial x} = \frac{\alpha}{x} \left[Pe \left(\frac{2-m}{3} \eta f_0' - \frac{m+1}{3} f_0 \right) \right]^{1/2}$$

which follow from equation (2).

At neutral stability, the vortex mode of the three-dimensional disturbances are of the form[13, 14]

$$\begin{aligned} \psi_1(x, y, z) &= \hat{\psi}(x, y) \exp[iaz], \\ u_1(x, y, z) &= \hat{u}(x, y) \exp[iaz], \\ T_1(x, y, z) &= \hat{T}(x, y) \exp[iaz], \end{aligned} \tag{38}$$

where a is the spanwise periodic wave number which is real. Substituting equation (38) into equations (35)–(37) yields

$$ia\hat{u} = \frac{\partial^2 \hat{\psi}}{\partial x \partial y}, \tag{39}$$

$$\left(\frac{\partial^2 \hat{\psi}}{\partial y^2} - a^2 \hat{\psi} \right) = -\frac{iK \rho_\infty \beta g a \hat{T}}{\mu}, \tag{40}$$

$$\alpha \left(\frac{\partial^2 \hat{T}}{\partial y^2} - a^2 \hat{T} \right) = u_0 \frac{\partial \hat{T}}{\partial x} + v_0 \frac{\partial \hat{T}}{\partial y} + \hat{u} \frac{\partial T_0}{\partial x} - ia\hat{\psi} \frac{\partial T_0}{\partial y}. \tag{41}$$

Equations (39)–(41) admit local similarity solution of the form

$$\begin{aligned} \hat{\psi}(x, y) &= i\alpha \sqrt{(Pe)}\, F(\eta, x), \\ \hat{u}(x, y) &= \frac{\alpha}{x} \sqrt{(Pe)}\, G(\eta, x), \\ \hat{T}(x, y) &= A x^m \Theta(\eta, x), \end{aligned} \tag{42}$$

where $F(\eta, x)$, $G(\eta, x)$ and $\Theta(\eta, x)$ are determined from

$$kG - \frac{1}{3} \left[(m-2)\eta \frac{\partial^2 F}{\partial \eta^2} + (2m-1) \frac{\partial F}{\partial \eta} \right] = x \frac{\partial^2 F}{\partial x \partial \eta}, \tag{43}$$

$$\left(\frac{\partial^2}{\partial \eta^2} - k^2 \right) F = -M(Pe)^{1/2} k\Theta, \tag{44}$$

$$\left(\frac{\partial^2}{\partial \eta^2} - k^2 \right) \Theta = m f_0' \Theta - \frac{m+1}{3} f_0 \frac{\partial \Theta}{\partial \eta} + (Pe)^{-1/2} \times \left(\frac{m-2}{3} \eta \Theta_0' + m\theta_0 \right) G + (Pe)^{1/2} \theta_0' kF + f_0' x \frac{\partial \Theta}{\partial x}, \tag{45}$$

where $k = ax/(Pe)^{1/2}$ is the dimensionless wave number. It is assumed that, after recasting in the similarity variable η, the x-dependence of the variables is weak such that $(\partial/\partial x) \ll (\partial/\partial \eta)$; then, the last terms in equations (43) and (45) are of higher order in their respective equations and therefore can be neglected. Equations (43)–(45) can then be simplified to give

$$G = \frac{1}{3k} [(m-2)\eta D^2 F + (2m-1) DF], \tag{46}$$

$$(D^2 - k^2) F = -M(Pe)^{1/2} k\Theta, \tag{47}$$

$$(D^2 - k^2)\Theta = m f_0' \Theta - \left(\frac{m+1}{3} \right) f_0 D\Theta + (Pe)^{-1/2} \left[\frac{m-2}{3} \eta \theta_0' + m\theta_0 \right] G + (Pe)^{1/2} \theta_0' kF, \tag{48}$$

subject to boundary conditions

$$F(0, x) = F(\infty, x) = 0, \tag{49}$$

$$\Theta(0, x) = \Theta(\infty, x) = 0, \tag{50}$$

where $D = \mathrm{d}/\mathrm{d}\eta$. The dependence of F, G, and Θ on x in equations (46)–(50) is only parametric, i.e. F, G, and Θ can be regarded as functions of η only. The assumption of the weak x-dependence and the resulting solutions have been called the "local similarity" solutions[19–21]. Note that $M = 0$ is for the case of forced convection in a porous medium. Substituting G from equation (46) and Θ from equation (47) into equation (48) yields the following equation in terms of F

$$(D^2 - k^2)^2 F + \left(\frac{m+1}{3} \right) f_0 D(D^2 - k^2) F + \frac{M}{3} \left[\frac{m-2}{3} \eta \theta_0' + m\theta_0 \right] - m f_0' (D^2 - k^2) F \times [(m-2)\eta D^2 F + (2m-1) DF] + MPe\, \theta_0' k^2 F = 0, \tag{51}$$

subject to the boundary conditions

$$F(0) = D^2 F(0) = 0, \tag{52}$$

$$F(\infty) = D^2 F(\infty) = 0. \tag{53}$$

For a set of values of m, M and k, equation (51) with boundary conditions given by equations (52) and (53) constitutes an eigenvalue problem where Pe can be regarded as the eigenvalue.

3. NUMERICAL SOLUTION OF THE EIGENVALUE PROBLEM

The eigenvalue problem can best be solved numerically by integrating equation (51) inward from $\eta \to \infty$ (i.e. the edge of the boundary layer of the basic flow) to $\eta = 0$ (at the wall). To start the numerical integration at $\eta \to \infty$, asymptotic solutions for the basic and disturbed flow will now be sought.

Consider first the asymptotic solutions for the basic flow. With the aid of equation (7a), equation (4) can be integrated twice to give

$$f_0 = \eta_\infty + B_0 \tag{54}$$

where B_0 is a measure of the amount of fluid entrained into the boundary layer induced by free convection. Substituting equation (54) into equation (5), we have

$$\theta_0'' + \sqrt{\left(\frac{m+1}{3}\right)}\xi\theta_0' - m\theta_0 = 0, \tag{55}$$

which has the solution

$$\theta_0 = A_0 \mathrm{e}^{-\xi^2/4} D_\nu(\xi), \tag{56}$$

and consequently

$$\theta_0' = -\sqrt{\left(\frac{m+1}{3}\right)} A_0 \mathrm{e}^{-\xi^2/4} D_{\nu+1}(\xi), \tag{57}$$

where $\xi \equiv \sqrt{[(m+1)/3]}(\eta_\infty + B_0)$, and A_0 is an integration constant. It should be noted that the boundary conditions at $\eta = 0$, i.e. equation (6a), cannot be imposed to equation (55) since the equation is valid only at η_∞. The asymptotic expansions for $\theta_0(\xi)$ and $\theta_0'(\xi)$ at $\xi \to \infty$ are

$$\theta_0(\xi) = A_0 \mathrm{e}^{-\xi^2/2}\xi^\nu\left\{1 - \frac{\nu(\nu-1)}{2\xi^2} + \frac{\nu(\nu-1)(\nu-2)(\nu-3)}{2\cdot 4\cdot \xi^4} \pm \cdots\right\}, \tag{58}$$

$$\theta_0'(\xi) = -\sqrt{\left(\frac{m+1}{3}\right)} A_0 \mathrm{e}^{-\xi^2/2}\xi^{\nu+1} \times\left\{1 - \frac{(\nu+1)\nu}{2\xi^2} + \frac{(\nu+1)\nu(\nu-1)(\nu-2)}{2\cdot 4\cdot \xi^4} \pm \cdots\right\}. \tag{59}$$

The improved approximations for f_0 and f_0' can now be obtained by the integration of equation (4) and with the aid of equations (58) and (59) to give

$$f_0 = \eta_\infty + B_0 + \frac{3M}{m+1} A_0 e^{-\xi^2/2}\xi^\nu \times\left\{\frac{(2-m)}{3} \frac{(2-m)}{3\xi}\sqrt{\left(\frac{m+1}{3}\right)} B_0 + \left[m + \left(\frac{2-m}{3}\right)\left(\frac{(\nu+1)(2-\nu)}{2} + \nu\right)\right]\Big/ \xi^2 \pm \cdots\right\}, \tag{60}$$

$$f_0' = 1 + \sqrt{\left(\frac{3}{m+1}\right)} M A_0 \mathrm{e}^{-\xi^2/2}\xi^{\nu+1} \times\left\{\frac{(2-m)}{3} - \frac{(2-m)}{3\xi}\sqrt{\left(\frac{m+1}{3}\right)} B_0 + \left[m + \left(\frac{2-m}{3}\right)\left(\frac{(\nu+1)(2-\nu)}{2}\right)\right]\Big/ \xi^2 \pm \cdots\right\}. \tag{61}$$

The numerical solutions for the basic flow can now be proceeded by guessing the values of A_0 and B_0 and evaluating θ_0, θ_0', f_0, and f_0' at $\eta = \eta_\infty$ from equations (58)–(61), which are used as the initial values for the Runge–Kutta integration procedure to integrate backward to $\eta = 0$. The boundary conditions at the end point given by equation (6) will then be tested, and the values of A_0 and B_0 will be adjusted based on the Newton–Raphson iteration method until equations (6a, b) are satisfied. The numerical results obtained in this way for the basic flow agree with the straightforward shooting method used by Cheng[17]. It is believed, however, the present method is superior because the boundary conditions at $\eta = \eta_\infty$ are exactly satisfied and that the values chosen for η_∞ are not required to be considerably larger than the boundary layer thickness. As a result, the required number of integration steps is reduced and the numerical procedure is stabilized.

Attention is next given to the asymptotic behavior of F. As $\eta \to \infty$ equation (51) reduces to

$$(D^2 - k^2)^2 F + \left(\frac{m+1}{3}\right)(\eta_\infty + B_0) D(D^2 - k^2)F - m(D^2 - k^2)F = 0, \tag{62}$$

where we have made use of boundary condition (7a) and equation (54). Hence, from the boundary condition (53) we have

$$(D^2 - k^2)F = C_2 \mathrm{e}^{-\xi^2/4} D\hat{v}(\xi), \tag{63}$$

where $\hat{v} = -(4m + 1 + 3k^2)/(m+1)$. Solving for F from equation (63) and imposing boundary conditions (53) gives

$$F(\eta_\infty) = C_1 \mathrm{e}^{-k\eta_\infty} + C_2 \int_{a_1}^{\eta_\infty} \mathrm{e}^{-k(\eta_\infty - \eta_1)} \times \int_{a_2}^{\eta_1} \mathrm{e}^{-k(\eta_2 - \eta_1)} \mathrm{e}^{-\xi_2^2/4} D_{\hat{v}}(\xi_2)\mathrm{d}\eta_2\,\mathrm{d}\eta_1, \tag{64}$$

where a_1 and a_2 are arbitrary constants, and $\xi_2 = \xi(\eta_2)$ with η_1 and η_2 denoting the dummy variables. We shall designate $F_1(\eta_\infty)$ and $F_2(\eta_\infty)$ as

$$F_1(\eta_\infty) = \mathrm{e}^{-k\eta_\infty}, \tag{65}$$

$$F_2(\eta_\infty) = \int_{a_1}^{\eta_\infty} \mathrm{e}^{-k(\eta_\infty - \eta_1)} \int_{a_2}^{\eta_1} \mathrm{e}^{-k(\eta_2 - \eta_1)} \mathrm{e}^{-\xi_2^2/4} D_{\hat{v}}(\xi_2)\mathrm{d}\eta_2\,\mathrm{d}\eta_1. \tag{66}$$

The two eigenfunctions for equation (48) are $F_1(\eta)$ and $F_2(\eta)$ whose linear combination is

$$F(\eta) = C_1 F_1(\eta) + C_2 F_2(\eta) \tag{67}$$

where the asymptotic functions for F_1 and F_2 are given by equations (65) and (66) respectively. The values of $F_1(\eta_\infty)$, $DF_1(\eta_\infty)$, $D^2F_1(\eta_\infty)$, and $D^3F_1(\eta_\infty)$ can now be found from equation (65). Similarly, the values of $F_2(\eta_\infty)$ and its derivatives can be obtained from

equation (66). For simplicity, we choose $a_1 = a_2 = \eta_\infty$ so that $F_2(\eta_\infty) = DF_2(\eta_\infty) = 0$. Hence, $D^2F_2(\eta_\infty)$ and $D^3F_2(\eta_\infty)$ can be found from

$$D^2F_2 = e^{-\xi^2/4} D_{\hat{\nu}}(\xi), \tag{68}$$

and

$$D^3F_2 = -\sqrt{\left(\frac{m+1}{3}\right)} e^{-\xi^2/4} D_{\hat{\nu}+1}(\xi), \tag{69}$$

which have similar asymptotic behavior as θ_0 and θ_0' as given by equations (56) and (57). Substituting equation (67) into equation (52) yields

$$\Delta(Pe; m, M, k) = F_1(0)D^2F_2(0) - F_2(0)D^2F_1(0) = 0. \tag{70}$$

For a given set of values of m, M, and k, condition (70) in general is not compatible unless Pe is the eigenvalue of the problem. To search for the eigenvalue Pe at fixed values of m, M, and K, the numerical procedure can be proceeded as follows. Using $F_i(\eta_\infty)$, $DF_i(\eta_\infty)$, $D^2F_i(\eta_\infty)$, and $D^3F_i(\eta_\infty)$ with $i = 1, 2$ as the starting values, the two paths of numerical integration were performed inward to $\eta = 0$ by means of the fourth-order Runge–Kutta method to obtain $F_i(0)$ and $D^2F_i(0)$. The first path is for $F_2(\eta)$ and the second path for $F_1(\eta)$. The Kaplan filtering technique[22] was applied during the second path of integration to ensure that the numerical results of $F_1(\eta)$ and $F_2(\eta)$ are linearly independent. A systematic iteration of Pe was made on the basis of the Newton–Raphson method until the condition (70) is satisfied to within acceptable accuracy.

4. RESULTS AND DISCUSSION

Numerical solutions for the eigenvalue problem, equation (51) with boundary conditions (52) and (53), are obtained for the two cases with $m = 0.5$ ($n = 0$) and $m = 2$ ($n = 1$) at selected values of M. Figure 2 shows the neutral stability curves for (i) a horizontal aiding flow over an impermeable surface with constant heat flux ($m = 0.5$ and $n = 0$), and (ii) stagnation point flow with $T_w \propto x^2$ ($m = 2$ and $n = 1$). The minimum values of Pe are the critical values for the onset of vortex instability. The values of the critical Peclet numbers and the associated wave numbers at various values of M are also tabulated in Table 1 for future reference. Note that the small values of Pe^* at large M in Table 1 do not indicate the failure of our scaling argument based on boundary layer approximations. Actually, when M is large (i.e. nearly free convection limit), the condition for the scaling argument is $Ra^{1/3} = M^{1/3}Pe^{1/2} \gg 1$.

The critical Peclet numbers and the associated dimensionless wave numbers as a function of the mixed convection parameter M are plotted in Figs. 3 and 4 respectively. The asymptotes for pure free and pure forced convective flows are also plotted in the same graph for comparison. The asymptotes for pure free convection are obtained from Hsu, Cheng and Homsy[13] who found that the critical Rayleigh numbers Ra_x^* and the associated wave number k_f^* for the onset of vortex instability in a porous medium adjacent to horizontal surfaces are

$$Ra_x^* = 59.78 \quad \text{and} \quad k_f^* = 0.81 \quad \text{for } m = 0.5,$$

$$Ra_x^* = 128.63 \quad \text{and} \quad k_f^* = 1.14 \quad \text{for } m = 2,$$

which can be rewritten as

$$Pe^* = 15.23(M)^{-2/3} \quad \text{and} \quad k^* = 0.81(M)^{1/3} \quad \text{for } m = 0.5,$$

$$Pe^* = 25.48(M)^{-2/3} \quad \text{and} \quad k^* = 1.14(M)^{1/3} \quad \text{for } m = 2,$$

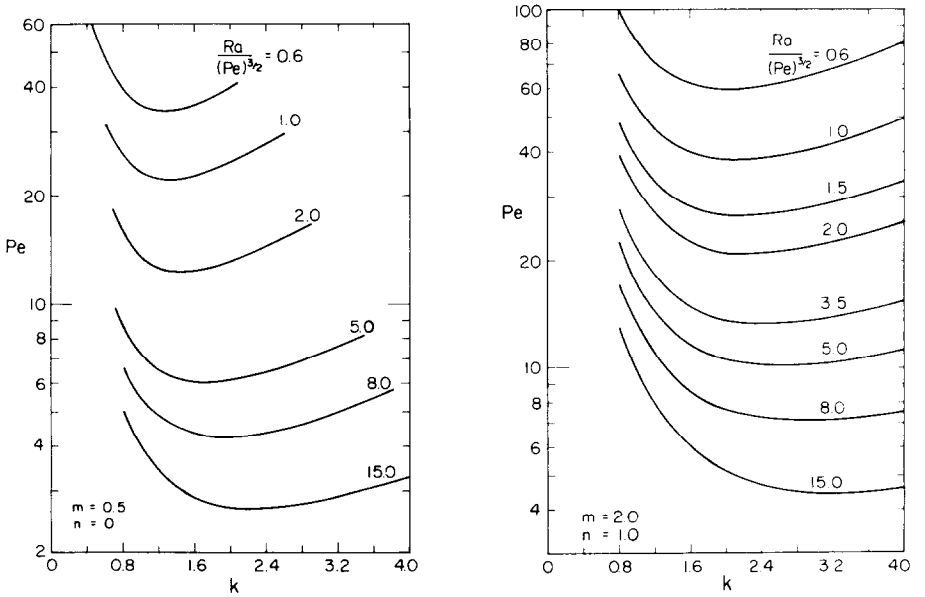

FIG. 2. Neutral stability curves for (a) flow past a horizontal impermeable surface with constant heat flux ($m = 0.5$ and $n = 0$) and (b) stagnation point flow about a horizontal impermeable surface with $T_w \propto x^2$ ($m = 2$ and $n = 1$).

Table 1. Critical Peclet numbers and their associated wave numbers

$Ra/(Pe)^{3/2}$	Flow past a horizontal plate ($m = 0.5$ and $n = 0$) Pe^*	k^*	Stagnation point flow about a horizontal plate ($m = 2.0$ and $n = 1.0$) Pe^*	k^*
0.2	96.42	1.17	168.2	1.93
0.4	50.21	1.21	87.05	1.97
0.6	34.68	1.25	59.83	2.02
1.0	22.09	1.31	37.84	2.09
2.0	12.34	1.44	20.92	2.25
5.0	6.01	1.71	10.07	2.59
8.0	4.23	1.91	7.07	2.85
15.0	2.68	2.24	4.47	3.28

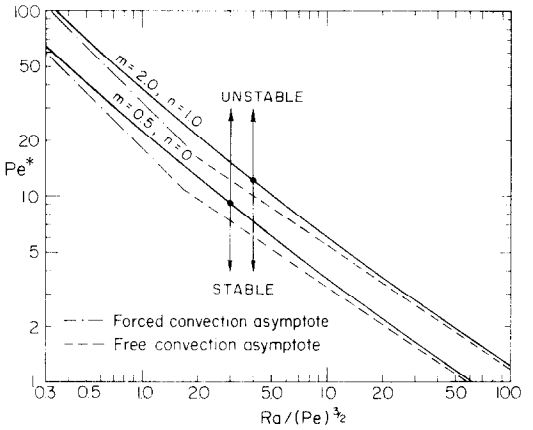

FIG. 3. Critical Peclet numbers vs mixed convection parameter $Ra/(Pe)^{3/2}$.

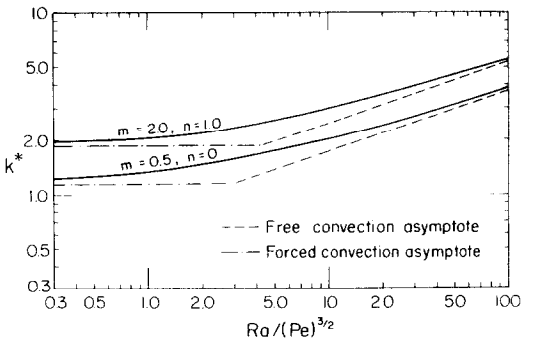

FIG. 4. Critical wave numbers vs mixed convection parameter $Ra/(Pe)^{3/2}$.

where we have used the relations $Pe = (Ra/M)^{2/3}$ and $k^* = k_f^*(M)^{1/3}$. The asymptotes for nearly pure forced convection are obtained by letting $M \to 0$ in equation (51) while regarding MPe as the eigenvalue of the problem. The numerical computation for this case yields

$$Pe^* = 18.38(M)^{-1} \quad \text{and} \quad k^* = 1.13 \quad \text{for } m = 0.5,$$

and

$$Pe^* = 32.34(M)^{-1} \quad \text{and} \quad k^* = 1.88 \quad \text{for } m = 2.$$

The finite values of MPe^* imply that $Pe^* \to \infty$ as $M \to 0$, indicating forced convective flow about horizontal surfaces is stable to vortex instability.

It is interesting to note that the neutral stability curves for combined free and forced convection lie above the asymptotes for pure free and nearly pure forced convection. (Fig. 3). When the value of M increases from $M = 0$, the combined free and forced convection flow has a higher critical Pe^* than the pure forced convection flow (with $M = 0$), indicating the stabilizing effect of the term $u_1(\partial T_0/\partial x)$ which becomes negligible as $M \to 0$. On the other hand, when M decreases from $M \to \infty$, the combined free and forced convection flow has a higher critical Pe than the pure free convection flow (with $M \to \infty$), indicating that the increase in the free stream velocity tends to stabilize the flow; this is consistent with the results obtained by Hsu *et al.*[13] who found that the inclusion of the term $u_0(\partial T_1/\partial x)$ in the perturbation equations has stabilized the flow. The neutral stability curve for $m = 2$ (stagnation point flow) lies above that for $m = 0.5$ (flow over a horizontal surface) and is therefore more stable for the vortex mode of instability. This is as expected since the magnitude of the transverse velocity toward the wall inside the boundary layer for the case of the stagnation point flow (with $m = 2$) is much larger than the corresponding case of a horizontal aiding flow (with $m = 0.5$) (see[17]). The larger transverse (inward-directed) velocity for the stagnation point flow tend to suppress the growth of disturbances[23].

5. CONCLUDING REMARKS

The present analysis is based on the assumptions that (i) Darcy's law is applicable for non-isothermal flow in porous media, (ii) the boundary layer approximations can be invoked to obtain the similarity solutions for the base flow. From previous theoretical and experimental studies[1,2], it is known that the first assumption is applicable if the Reynolds numbers (based on the square root of permeability) are less than one and if the ratio of permeability of the medium to the square of the characteristic length is small. For the second assumption, recent experiments by Evans and Plumb[24] on free convection boundary layers ad-

jacent to a vertical flat plate show that results based on similarity solutions agree well with experimental data for moderately large Rayleigh numbers.

Acknowledgements — The second author (P.C.) would like to thank Professor T. S. Chen for helpful discussion. The support of the National Science Foundation on this work through Grant No. ENG 77-27527 is gratefully acknowledged.

REFERENCES

1. P. A. Witherspoon, S. P. Neumann, M. L. Sorey and M. J. Lippmann, Modelling geothermal systems, Report No. 3263, Lawrence Berkeley Laboratory (1975).
2. P. Cheng, Heat transfer in geothermal systems, *Adv. Heat Transf.* **14,** 1–105 (1978).
3. E. R. Lapwood, Convection of a fluid in a porous medium, *Proc. Camb. Phil. Soc.* **44,** 508–521 (1948).
4. Y. Katto and T. Masuoka, Criterion for the onset of convective flow in a fluid in a porous medium, *Int. J. Heat Mass Transfer* **10,** 297–307 (1967).
5. D. R. Kassoy and A. Zebib, Variable viscosity effects on the onset of convection in porous media, *Physics Fluids* **18,** 1649–1651 (1975).
6. K. Walker and G. M. Homsy, A note on convective instabilities in Boussinesq fluids and porous media, *J. Heat Transfer* **99,** 338–339 (1977).
7. J. L. Beck, Convection in a box of porous material saturated with fluid, *Physics Fluids* **15,** 1377–1383 (1972).
8. S. A. Bories and M. A. Combarnous, Natural convection in a sloping porous layer, *J. Fluid Mech.* **57,** 63–70 (1973).
9. R. A. Wooding, Rayleigh instability of a thermal boundary layer in flow through a porous medium, *J. Fluid Mech.* **9,** 183–192 (1960).
10. F. M. Sutton, Onset of convection in a porous medium with net through flow, *Physics Fluids* **13,** 1931–1932 (1970).
11. G. M. Homsy and A. E. Sherwood, Convective instabilities in porous media with through flow, *A.I.Ch.E. Jl* **22,** 168–174 (1976).
12. A. E. Gill, A proof that convection in a porous vertical slab is stable, *J. Fluid Mech.* **35,** 545–547 (1969).
13. C. T. Hsu, P. Cheng and G. M. Homsy, Instability of free convection flow over a horizontal impermeable surface in a porous medium, *Int. J. Heat Mass Transfer* **21,** 1221–1228 (1978).
14. C. T. Hsu and P. Cheng, Vortex instability in buoyancy-induced flow over inclined heated surfaces in porous media, *J. Heat Transfer* **101,** 660–665 (1979).
15. S. E. Haaland and E. M. Sparrow, Vortex instability of natural convection flow on inclined surfaces, *Int. J. Heat Mass Transfer* **16,** 2355–2367 (1973).
16. G. J. Hwang and K. C. Cheng, Convective instability of laminar natural convection flow on inclined isothermal plates, *Can. J. Chem. Engng* **51,** 659–666 (1973).
17. P. Cheng, Similarity solutions for mixed convection from horizontal impermeable surfaces in saturated porous media, *Int. J. Heat Mass Transfer* **20,** 893–898 (1977).
18. W. Magnus and F. Oberthettinger, *Functions of Mathematical Physics*, pp. 91–94 (translated by J. Wermer. Chelsea Publishing Company, New York (1949).
19. F. K. Moore, *Theory of Laminar Flows*, pp. 486–490. Princeton University Press (1964).
20. E. M. Sparrow and H. S. Yu, Local non-similarity thermal boundary layer solutions, *J. Heat Transfer* **93,** 328–334 (1971).
21. E. M. Sparrow, H. Quack and C. J. Boerner, Local nonsimilarity boundary layer solutions, *AIAA Jl* **8,** 1936–1942 (1970).
22. R. E. Kaplan, The stability of laminar incompressible boundary layers in the presence of compliant boundaries, M.I.T. Aero-Elastic and Structures Research Laboratory, ASRL-TR 116-1 (1964).
23. F. K. Tsou and E. M. Sparrow, Hydrodynamic stability of boundary layers with mass transfer, *Appl. Scient. Res.* **22,** 273–286 (1970).
24. G. H. Evans and O. A. Plumb, Natural convection from a vertical isothemmal surface imbedded in a saturated porous medium, Thermophysics and Heat Transfer Conference, Palo Alto, California, May 24–26, AIAA-ASME Paper No. 78-HT-55, 1978.

INSTABILITE TOURBILLONNAIRE DE LA CONVECTION MIXTE DANS UN MILIEU POREUX SEMI-INFINI LIMITE PAR UNE SURFACE HORIZONTALE

Résumé—Par une analyse linéaire de stabilité, on détermine les conditions d'apparition des tourbillons longitudinaux pour les écoulements de convection mixte dans un milieu poreux semi-infini limité par une surface imperméable et horizontale. On considère deux écoulements différents: (1) écoulement sur une surface imperméable horizontale avec un angle d'incidence nul, (2) écoulement autour du point d'arrêt sur une surface horizontale. Dans chaque problème, on suppose une couche limite bidimensionnelle caractérisée par des profils non linéaires de vitesse et de température. Les équations aux perturbations tridimensionnelles sont simplifiées à partir d'un argument d'échelle et les équations simples résultantes sont résolues à partir d'une méthode de similitude locale. Le nombre de Péclet critique et le nombre d'onde associé sont obtenus dans les deux cas en fonction du paramètre de convection mixte. En ce qui concerne le mode d'instabilité tourbillonnaire, on trouve que l'écoulement à point d'arrêt est plus stable que l'autre pour la même valeur du paramètre. Dans les deux cas, l'effet de l'écoulement externe est de supprimer l'apparition de l'instabilité tourbillonnaire dans la couche poreuse adjacente à la surface horizontale.

WIRBELINSTABILITÄT EINER GEMISCHTEN KONVEKTIONSSTRÖMUNG IN EINEM HALBUNENDLICHEN, PORÖSEN MEDIUM, WELCHES DURCH EINE HORIZONTALE OBERFLÄCHE BEGRENZT IST

Zusammenfassung—Es wird eine lineare Stabilitätsanalyse durchgeführt, um die Bedingungen für das Auftreten von Längswirbeln in gemischten Konvektionsströmungen in einem halbunendlichen, porösen Medium zu bestimmen, das an eine ebene, undurchlässige Oberfläche grenzt. Zwei verschiedene Hilfsströmungen werden betrachtet: (1) die Strömung hinter einer horizontalen, undurchlässigen Oberfläche mit Nullanstellwinkel und (2) die Staupunktströmung um eine horizontale Oberfläche. Für jedes Problem wird für den Grundzustand die stationäre zweidimensionale Grenzschichtströmung angenommen, die durch nichtlineare Geschwindigkeits- und Temperaturprofile gekennzeichnet ist. Die instationären dreidimensionalen Störungsgleichungen werden auf der Grundlage eines Maßstabsfaktors vereinfacht, und die sich ergebenden vereinfachten Gleichungen werden mit Hilfe der Methode der örtlichen Ähnlichkeit gelöst. Die kritischen Peclet-Zahlen und die zugehörigen Wellenzahlen werden als Funktionen des Parameters der gemischten Konvektion erhalten. Für die Wirbelform der Instabilität wurde gefunden, daß die Staupunktströmung stabiler als die horizontale Hilfsströmung für den gleichen Wert des Strömungsparameters ist. In beiden Fällen soll die Wirkung der äußeren Hilfsströmung den Beginn der Wirbelinstabilität in der porösen Schicht, die an die horizontale Oberfläche angrenzt, unterdrücken.

ВИХРЕВАЯ НЕУСТОЙЧИВОСТЬ СМЕШАННОЙ КОНВЕКЦИИ В ПОЛУБЕСКОНЕЧНОЙ ПОРИСТОЙ СРЕДЕ, ОГРАНИЧЕННОЙ ГОРИЗОНТАЛЬНОЙ ПОВЕРХНОСТЬЮ

Аннотация — Выполнен анализ линейной устойчивости с целью определения условий возникновения продольных вихрей в смешанных конвективных потоках в полубесконечном пористом слое, прилегающем к горизонтальной непроницаемой поверхности. Рассмотрены два типа течения: (1) у горизонтальной непроницаемой поверхности при нулевом угле натекания и (2) в критической точке у горизонтальной поверхности. В каждой из задач предполагается, что основным режимом является стационарное двумерное течение в пограничном слое, характеризующееся нелинейными профилями скорости и температуры. Уравнения нестационарных трехмерных возмущений упрощаются за счет введения масштаба и решаются методом локального подобия. Для двух случаев получены значения критического числа Пекле и соответствующие волновые числа в зависимости от параметра смешанной конвекции. Установлено, что течение в критической точке является более устойчивым, чем вдоль горизонтальной поверхности при одном и том же значении параметра смешанной конвекции. В обоих случаях индуцированный поток гасит вихревую неустойчивость в пористом слое, прилегающем к горизонтальной ограничивающей поверхности.